Packing Motifs and Magneto-Structural Correlations in Crystal Structures of Metallo-Tetrakis(1,2,5-thiadiazole)porphyrazine Series, MTTDPz (M = H_2, Fe, Co, Ni, Cu, Zn)

Yosuke Suzuki, Masato Fujimori, Hirofumi Yoshikawa, and Kunio Awaga*[a]

Abstract: Single crystals of tetrakis(thiadiazole)porphyrazine and the corresponding metal(II) derivatives, MTTDPz (M = H_2, Fe, Co, Ni, Cu, and Zn) were grown by sublimation under reduced pressure with continuous N_2 gas flow. Their structures, obtained by X-ray crystallographic analysis, depend significantly on the central metal ion, and the M = Ni and Cu derivatives exhibit polymorphism. They can be classified into three forms, α, β, and γ. The α form (M = H_2, Ni, and Cu) is composed of two-dimensional hexagonal close packing formed by side-by-side contacts between thiadiazole rings, whereas the β form (M = Fe, Co, and Zn) crystallizes into a one-dimensional coordination polymer. The γ form (M = Ni and Cu) consists of a ladder structure caused by π stacking, similar to the β form of phthalocyanine, and by side-by-side contacts between thiadiazole rings. Although the crystal structures of the MTTDPz series exhibited multi-dimensional network structures, magnetic measurements revealed relatively weak exchange interactions, probably reflecting the long distances between the metal ions.

Keywords: crystal growth · magnetic properties · porphyrazines · solid-state structures · transition metals

Introduction

Phthalocyanine (MPc) compounds have been studied extensively in the last three decades because of their commercial applications including as dyes and catalysts. They have also attracted much interest due to their electric, electro-optic and magnetic properties.[1] Thin films of MPc are utilized as gas sensors; oxidizing gases such as NO_x, HCl, CO introduce mobile holes in MPc leading to a significant enhancement in conductivity.[1,2] MnPc[3] and FePc[4] possess ferromagnetically ordered states at low temperatures and $[N(C_4H_9)_4][Ln(Pc)_2]$ exhibits the behavior of a single-molecule magnet.[5]

There are two well-known crystal forms for MPc, α, and β.[6,7] Both forms consist of a one-dimensional stacking column, in which the molecules have a large π–π overlap. In contrast, intercolumn interactions appear to be hindered by the terminal hydrogen atoms on the benzo ring. Such low dimensionality must be disadvantageous for three-dimensional electrical conduction. Seeking multi-dimensional interactions, Inabe et al. studied the $MPc(CN)_2$ series. In this series, the cyanide ions, bonding to the central metal ions, brought about partial face-to-face overlap of the Pc rings instead of eclipsed overlap. This resulted in multi-dimensional π–π interaction in $K[CoPc(CN)_2]_2{\cdot}5\,CH_3CN$ and other derivatives.[8,9] Ercolani et al. synthesized tetrakis(thiadiazole)porphyrazine (TTDPz) and the corresponding metal(II) derivatives, MTTDPz (M = H_2, Mg, Mn, Fe, Co, Ni, Cu, and Zn),[10,11] in which intermolecular interactions of the thiadiazole ring were strongly expected in the solid state. However, no structural data on the MTTDPz series has been reported to date, although crystal structures of asymmetric, related compounds have been reported.[12,13]

In the present work we grew crystals of the MTTDPz series (M = H_2, Fe, Co, Ni, Cu, Zn) and performed structural analysis and magnetic measurements. Although we have briefly reported the structures of H_2TTDPz and CoTTDPz,[14] herein we describe in detail the crystal structures of the MTTDPz series. Based on these data, packing motifs and magneto-structural correlations will be discussed.

Results and Discussion

Crystal growth and structure: The materials MTTDPz (M = H_2, Mn, Fe, Co, Ni, Cu, and Zn) were prepared by the literature method.[10,11] Single crystals were obtained by sublimation under reduced pressure with continuous N_2 gas flow, though growth of MnTTDPz crystals was unsuccessful.

---

[a] Y. Suzuki, M. Fujimori, Dr. H. Yoshikawa, Prof. K. Awaga
Department of Chemistry, Graduate School of Science
Nagoya University, Furo-cho, Chikusa-ku
Nagoya 464–8602 (Japan)
Fax: (+81) 52-789-2484
E-mail: awaga@mbox.chem.nagoya-u.ac.jp

DOI: 10.1002/chem.200400394

The structures of the obtained crystals were determined by X-ray crystallographic analyses. The details are described in the Experimental Section. It is notable that X-ray quality crystals could not been grown without N_2 gas flow.

The structures of the MTTDPz series can be broadly classified into three forms: α, β, and γ, as listed in Table 1. Their crystallographic data are summarized in Table 2. Figure 1 shows photographs of the three crystal forms. The α and β forms crystallized into block crystals in contrast to needle crystals for the γ form, which was easily distinguishable from the other two. The α form was observed in the H_2, Ni, and Cu derivatives. Since the structure of CuTTDPz is slightly different from those of the other two, it will be hereafter denoted as α′. The β form was observed in the Fe, Co, and Zn derivatives, and the γ form in the Ni and Cu derivatives. Therefore, the Ni and Cu derivatives exhibited the polymorphs α (or α′) and γ. The two forms of NiTTDPz were separately prepared by controlling the sublimation temperature: 450 °C for the α form and 500 °C for γ. However, a mixture of α′ and γ forms of CuTTDPz was always obtained by sublimation of $Cu(H_2O)_2TTDPz$ prepared from MgTTDPz, whereas only the γ form was obtained by sublimation of $Cu(py)_2TTDPz$ (py = pyridine) prepared from reaction of H_2TTDPz with copper acetate in pyridine. The α′ crystals were separated under a microscope for crystallographic analysis and magnetic measurements.

Table 1. Crystal forms for the MTTDPz series.

M =	H_2	Fe	Co	Ni	Cu	Zn
	α			α	α′	
		β	β			β
				γ	γ	

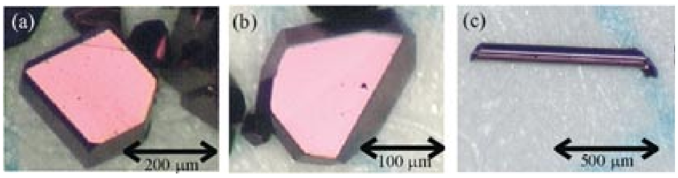

Figure 1. Crystals of the three forms of the MTTDPz series; α, β, and γ; a) α-NiTTDPz, b) β-ZnTTDPz, and c) γ-NiTTDPz.

The α form: This is the crystal form for the H_2, Ni, and Cu TTDPz derivatives, though the Ni and Cu derivatives exhibited polymorphism. The crystals of MTTDPz (M = H_2, Ni) belong to a monoclinic $P2_1/n$ space group, in which half of the molecule is crystallographically asymmetric. They have very similar lattice parameters.

Table 2. Crystallographic data for the MTTDPz series.

	α-H_2TTDPz	β-FeTTDPz	β-CoTTDPz	α-NiTTDPz
formula	$C_{16}H_2N_{16}S_4$	$C_{16}N_{16}S_4Fe$	$C_{16}N_{16}S_4Co$	$C_{16}N_{16}S_4Ni$
M_r	546.58	600.41	603.49	603.27
crystal system	monoclinic	monoclinic	monoclinic	monoclinic
space group	$P2_1/n$	$P2_1/c$	$P2_1/c$	$P2_1/n$
a [Å]	8.9250(3)	13.3190(12)	13.2660(4)	8.9340(3)
b [Å]	12.0340(5)	9.1110(8)	9.1170(3)	11.9920(6)
c [Å]	9.8650(4)	18.5590(17)	18.5140(5)	9.9011(4)
β [°]	116.500(2)	122.668(4)	122.382(2)	117.508(3)
V [Å^3]	948.21(6)	1895.9(3)	1890.99(10)	940.85(7)
Z	2	4	4	2
ρ [gcm^{-1}]	1.91	2.10	2.12	2.13
$\mu(Mo_{K\alpha})$ [mm^{-1}]	0.554	1.290	1.404	1.530
θ range [°]	4.10–29.88	4.26–25.00	4.27–29.90	4.12–27.93
used reflections	2715	3178	5194	2170
parameters	167	334	334	169
$R1$[a]	0.0419	0.0730	0.0392	0.0314
$wR2$	0.1019	0.1485	0.1024	0.0882
max/min [e Å^{-3}]	0.346/−0.330	1.263/−0.396	0.873/−0.934	0.532/−0.466
	γ-NiTTDPz	α′-CuTTDPz	γ-CuTTDPz	β-ZnTTDPz
formula	$C_{16}N_{16}S_4Ni$	$C_{16}N_{16}S_4Cu$	$C_{16}N_{16}S_4Cu$	$C_{16}N_{16}S_4Zn$
M_r	603.27	608.10	608.10	609.93
crystal system	monoclinic	monoclinic	monoclinic	monoclinic
space group	$P2_1/n$	$P2_1/c$	$P2_1/n$	$P2_1/c$
a [Å]	4.978(2)	23.97(3)	5.0240(2)	13.308(4)
b [Å]	21.063(8)	11.99(1)	21.1600(13)	9.283(3)
c [Å]	17.854(7)	26.64(3)	17.8770(14)	18.453(6)
β [°]	94.679(5)	102.80(1)	94.476(2)	122.878(4)
V [Å^3]	1865.8(13)	7466(14)	1894.7(2)	1914.5(10)
Z	4	16	4	4
ρ [gcm^{-1}]	2.15	2.16	2.13	2.12
$\mu(Mo_{K\alpha})$ [mm^{-1}]	1.543	1.673	1.648	1.773
θ range [°]	3.12–27.53	3.07–27.48	4.14–27.50	3.13–27.48
used reflections	4246	15756	3631	4343
parameters	334	1336	334	334
$R1$[a]	0.0424	0.0777	0.0518	0.0864
$wR2$	0.1014	0.2731	0.0944	0.1658
max/min [e Å^{-3}]	0.634/−0.585	1.395/−1.038	0.432/−0.409	0.955/−0.623

[a] Calculated using reflections of $F_o^2 > 2\sigma(F_o^2)$.

The structure of the α-form consists of a layered structure, of which the top and side views for NiTTDPz are shown in Figure 2a and b, respectively. The layer is formed by two-dimensional hexagonal close packing of NiTTDPz with very short S···N contacts of 2.925(2) and 3.247(2) Å. The corresponding distances are 2.948(2) and 3.245(2) Å in H_2TTDPz, and 2.900(5)–2.936(6) Å and 3.171(5)–3.213(6) Å in CuTTDPz. These distances are much shorter than the sum of the van der Waals radii of N and S (3.35 Å), indicating large intermolecular overlaps between π orbitals. The side view in Figure 2b shows that the layers stack along the c axis giving π–π interactions with an ABC repeat unit. Each layer is related by a twofold screw axis parallel to the b axis, with an interlayer distance of ~3.3 Å.

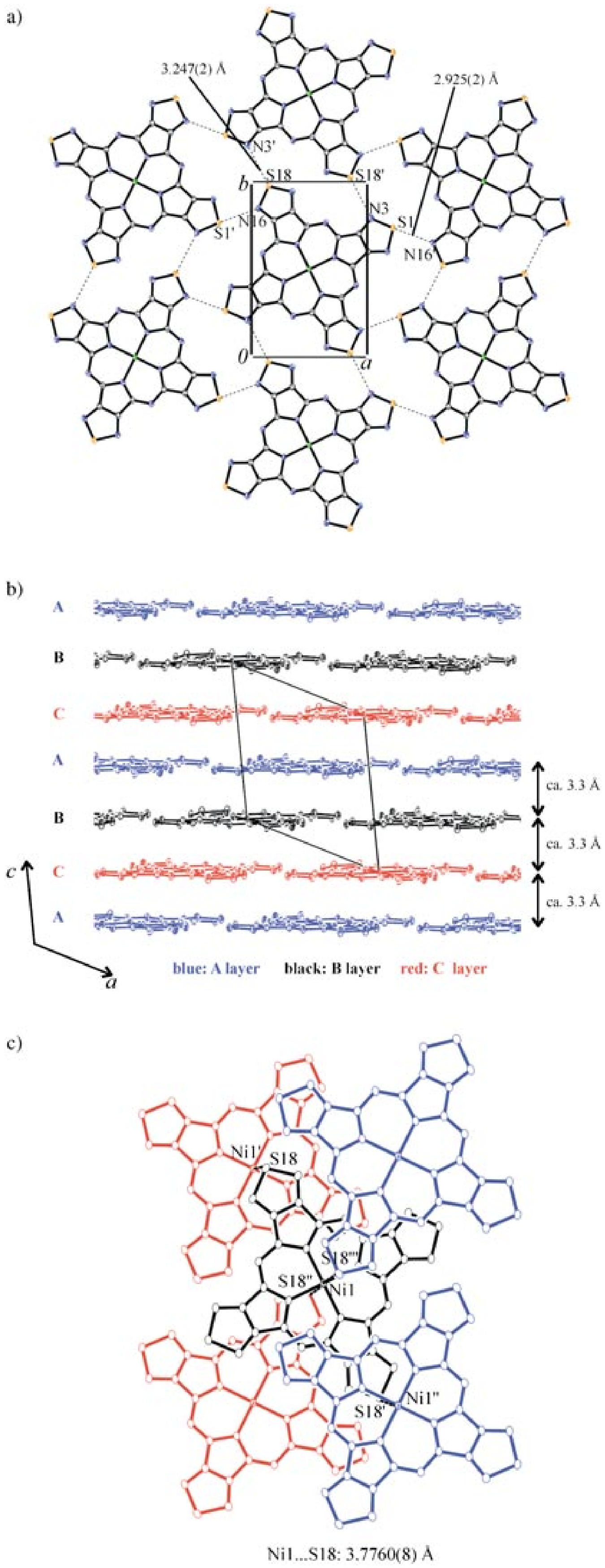

Figure 2. a) Top and b) side views of the layered crystal structure, and c) the intermolecular arrangement of the three repeating layers in α-NiTTDPz.

The stacking pattern and interlayer distance are similar to those of graphite.

Figure 2c depicts the intermolecular arrangement of the three neighboring layers that form the repeating pattern. One molecule in the middle layer interacts with two each in the upper and lower layers. The sulfur atom on the thiadiazole ring appears to occupy the axial position of the Ni ion with a distance of 3.7760(8) Å. However, the corresponding distance in metal-free H_2TTDPz, namely the distance between the molecular center and the sulfur atom, is 3.7631(2) Å, which is nearly identical to that of NiTTDPz. This indicates that the interlayer distance of the two compounds is not governed by metal–sulfur interactions, but by π–π interactions. This is reasonable given that Ni^{2+} ions (d^8) usually exhibit square-planar coordination without axial ligands.

The α′ crystal form of CuTTDPz belongs to a monoclinic $P2_1/c$ space group. The intralayer structure of α′-CuTTDPz is similar to that of the α form; however, there is a significant difference in interlayer arrangement. Figure 3 depicts the side view of the layered structure of α′-CuTTDPz, in which the asymmetric unit is composed of the three molecules labeled Cu1, Cu2, and Cu3, and two halves of the molecules labeled Cu4 and Cu5. The π stacking along the c axis has an ABAC repeat unit, in which the layers A, B, and C are formed by molecules Cu2 and Cu3, Cu1, and Cu4 and Cu5, respectively. The axial positions of the Cu^{2+} ions are occupied by nitrogen atoms from the thiadiazole rings with distances of ~3.6 Å. These distances are much shorter than those between the molecular center and the sulfur atom in H_2TTDPz and NiTTDPz, suggesting that the coordination bond between the nitrogen atom and the Cu ion contributes to the interlayer arrangement attaining the α′ form. Compared with the structures of α-H_2TTDPz and α-NiTTDPz, α′-CuTTDPz has a distorted layer structure of lower symmetry.

Epitaxial growth of MPc's have been extensively studied on various surfaces. It is believed that the arrangements of neighboring molecules on surfaces are governed by steric effects of the terminal hydrogen atoms on the benzo rings.[15] In contrast, the two-dimensional layered structure of the α form is caused by electrostatic attraction between the thiadiazole rings. This is a crucial difference between MPc and MTTDPz. The two-dimensional network present in the α form suggests application in the generation of oriented thin films.

The β form: FeTTDPz, CoTTDPz, and ZnTTDPz are isostructural and crystallize into the β form, which belongs to a monoclinic $P2_1/c$ space group. Each molecule is crystallographically independent. These three derivatives do not exhibit polymorphism.

Figure 4 depicts the molecular structure of ZnTTDPz, which is significantly different from those of FeTTDPz and CoTTDPz. The Zn ion is located above the porphyrazine plane by 0.394(3) Å, in contrast to the planar molecular structures of the other two. A similar displacement of the center metal ion out of the molecular plane has been observed in other metallophthalocyanines such as PbPc,[16]

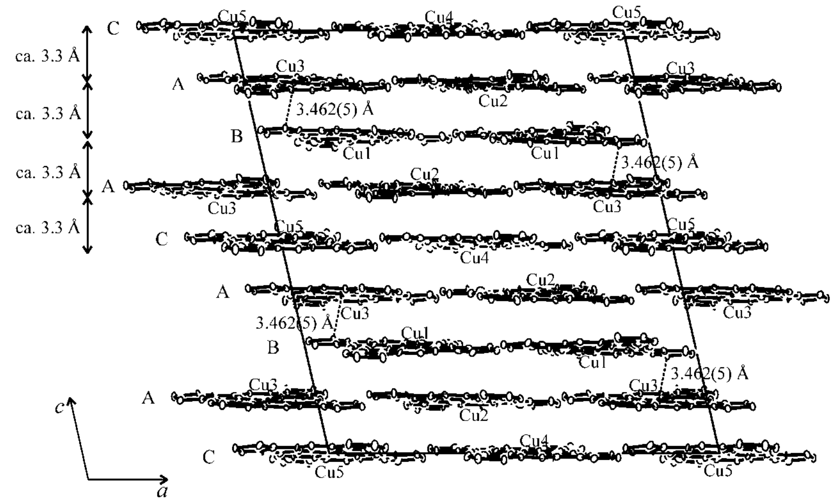

Figure 3. Side view of the layered crystal structure in α′-CuTTDPz.

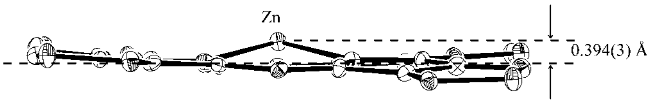

Figure 4. Molecular structure of β-ZnTTDPz.

SnPc,[17] and ZnPcX (X = amine, halogen, or other group).[18] The Pb and Sn ions are located above the molecular plane by 1.28 Å and 1.13 Å, respectively, probably reflecting their large ionic radii. In ZnPcX, the Zn ions are of square pyramidal five coordination and are ~0.5 Å above the planes, in contrast to the planar structure in ZnPc.[19] The molecular structure of ZnTTDPz is considered to occur through strong coordination bonding between the Zn^{2+} ion and the axial nitrogen.

Figure 5a depicts the structure of FeTTDPz, which forms a one-dimensional coordination polymer along the *b* axis. The nitrogen atom on the thiadiazole ring occupies the axial position of the metal ion in each neighboring molecule, and thus the metal ions are penta-coordinated. Each neighboring molecule in this chain is related by a twofold screw axis parallel to the *b* axis. The metal···nitrogen distances in β-MTTDPz (M = Fe, Co, and Zn) are 2.327(6), 2.300(2), and 2.187(5) Å, respectively. The shorter distance in ZnTTDPz is caused by the nonplanar molecular structure of this molecule. The dihedral angles between the neighboring molecular planes are 82.58(2)° in FeTTDPz, 82.96(1)° in CoTTDPz, and 85.45(2)° in ZnTTDPz. This type of edge-to-face interaction has previously been reported for zinc derivatives of the asymmetric porphyrazine.[20]

The coordination chains stack in the *bc* plane, leading to a two-dimensional network, as shown in Figure 5b. The interchain arrangements give rise to a face-to-face π dimer, of which the top and side views are shown in Figure 6a and b, respectively. The axial position of the Fe ion is occupied by the nitrogen atom of a pyrrole ring of the neighboring molecule, with a distance of 3.453(6) Å. The corresponding distances in CoTTDPz and ZnTTDPz are 3.401(2) and 3.783(5) Å, respectively. The intradimer Fe···Fe distance (4.066(2) Å) is much shorter than the shortest Fe···Fe distance in the coordination chain (7.361(2) Å). A magnetic interaction is expected in the dimer, occurring through the axial nitrogen atom. Furthermore, the two-dimensional network is stacked along the *a* axis with short S···N contacts between thiadiazole rings (not shown).

The γ form: The Ni and Cu derivatives crystallize into the γ form, which is of monoclinic $P2_1/n$ space group, although they also crystallize into the α form. The γ form consists of a two-leg ladder structure along the *a* axis. Figure 7a depicts a side view of this structure in γ-NiTTDPz. Figure 7b shows the intermolecular arrangements in the leg and row directions of the ladder. Along the leg direction, the molecular

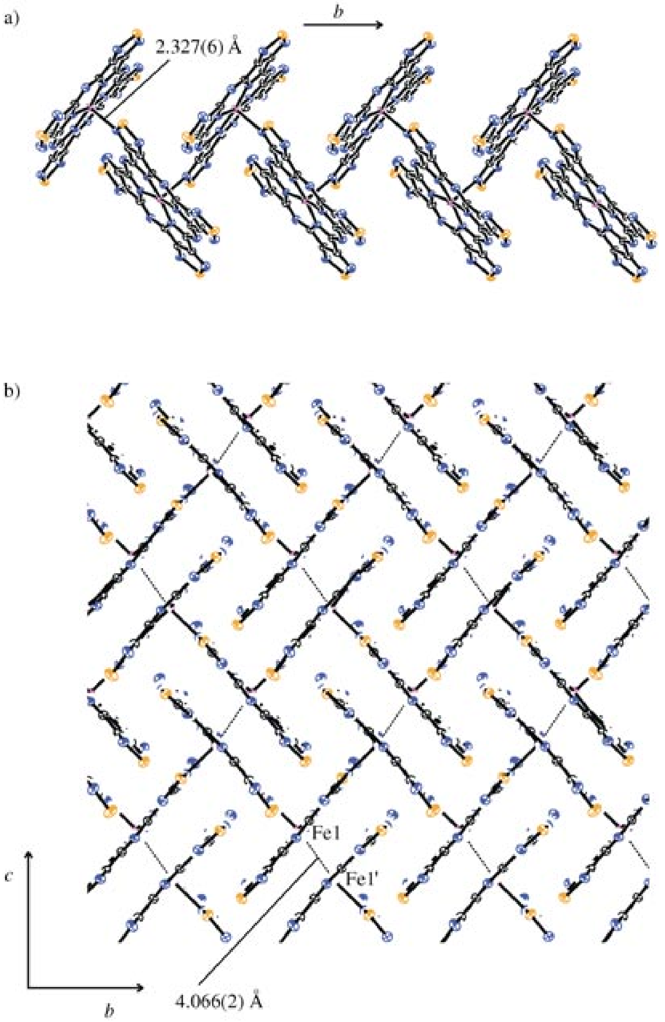

Figure 5. Views of the crystal structure in β-FeTTDPz; (a) coordination polymer along the *b* axis; (b) a projection onto the *bc* plane.

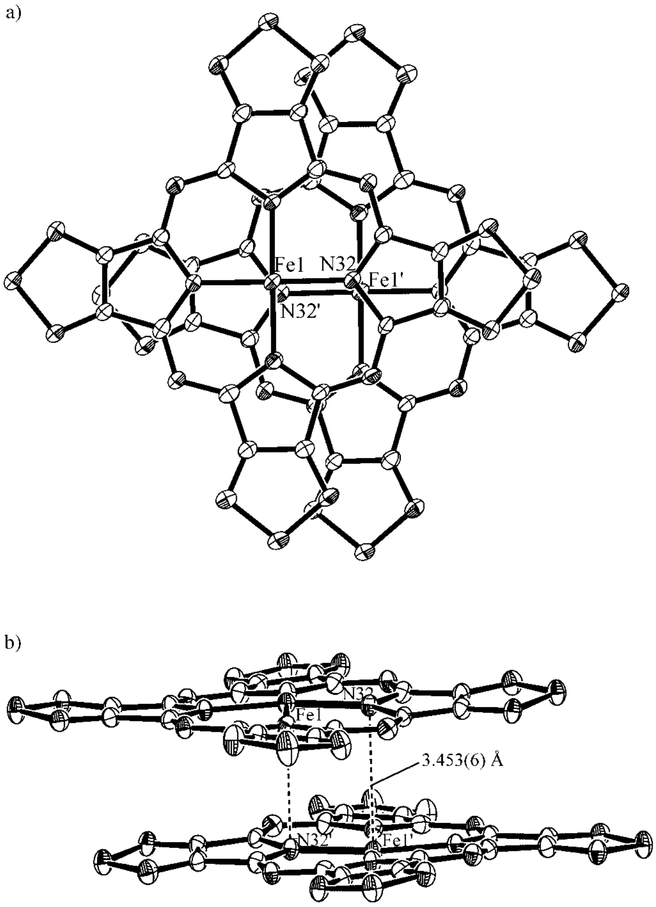

Figure 6. a) Top and b) side views of face-to-face π dimer in the interchain arrangement in β-FeTTDPz.

planes, tilted by about 40° with respect to this direction, stack with π–π overlap. The axial positions of the Ni ion are occupied by nitrogen atoms bridging the distance between the pyrrole rings on neighboring separate molecules. This chain includes a weak alternation such that there are two Ni···axial N distances of 3.177(3) and 3.298(3) Å. The structure of γ-CuTTDPz is very similar to that of γ-NiTTDPz with corresponding Cu···N distances of 3.196(4) and 3.271(4) Å. These stacking features are similar to those of the β form of MPc,[6,7] though there is no alternation in β-MPc. Along the row direction, the NiTTDPz molecules have side-by-side contact with a short S···N distance of 3.013(3) Å. The corresponding distance in CuTTDPz is 3.042(4) Å. They are shorter than the sum of the van der Waals radii. In this side-by-side dimer unit, the two molecules are related by an inversion center.

A projection of the crystal structure of γ-NiTTDPz along the *a* axis is shown in Figure 7c, in which the arrangement of four two-leg ladders is presented. There is a close S···N contact of 3.124(3) Å between the ladders in γ-NiTTDPz, while the corresponding distance in γ-CuTTDPz is 3.163(4) Å. In the γ form, the molecules are related by a twofold screw axis parallel to the *b* axis.

Packing motifs of MTTDPz: The structures of metal and metal-free phthalocyanines are well known to be almost independent of the central metal ions[6,7] with their structures governed by the π–π condensation energy of the planar molecules. In contrast, the structures of the MTTDPz series do depend on the central metal ions, and the S···N and π–π interactions of the thiadiazole ring also play significant roles in their solid structures. Since metal-free H_2TTDPz exhibits the α form, this structure is regulated by the π–π condensation energy. NiTTDPz and CuTTDPz do not form the β structure, which is a coordination polymer structure formed by bonding between the metal ion and the axial nitrogen atom. Absence of β-NiTTDPz and β-CuTTDPz can be explained by the fact that Ni^{2+} (d^8) and Cu^{2+} (d^9) are Jahn–Teller ions usually with lack of axial bonding or an elongated axial distance. There is no reason for H_2TTDPz to exhibit the β form. FeTTDPz, CoTTDPz, and ZnTTDPz crystallize into only the β form, which indicates that axial bonding is a driving force in generating the β form. Since NiTTDPz and CuTTDPz exhibit polymorphism between the α and γ forms, these forms should be energetically balanced.

It is concluded that the first driving force in the packing motif of the MTTDPz series is axial coordination between the metal ion and the nitrogen on the thiadiazole ring. This bonding brings about the β form. If central metal ion does not favor short axial bonding, MTTDPz molecules crystallize into the α or γ form.

Magnetic properties: The temperature dependence of magnetic susceptibility was examined for the M = Co (β form), Fe (β form), and Cu (α′and γ forms) derivatives. Paramagnetic susceptibilities (χ_p) were obtained by compensating for diamagnetic contributions. H_2TTDPz, NiTTDPz, and ZnTTDPz were diamagnetic. Figure 8 shows χ_p versus T plots for β-CoTTDPz and β-FeTTDPz. The values of χ_p for β-CoTTDPz increase gradually with decreasing temperature down to 12 K, and after attaining a rather sharp maximum at this temperature, χ_p quickly decreases to zero. For FeTTDPz, χ_p also increases with decreasing temperature from 300 K. However, χ_p does not exhibit a global maximum but instead a hump at 20 K. The sharp increase of χ_p below this temperature is probably caused by paramagnetic lattice defects displaying Curie behavior. According to the structure of the β form, the data for the two compounds were interpreted in terms of the antiferromagnetic dimer model [Eq. (1)],[21] in which N is the Avogadro constant, g is the g factor, S is the spin quantum number, J is the intradimer coupling constant, k_B is the Boltzmann constant, and C_{def} is the Curie constant for paramagnetic lattice defects.

$$\chi_p = \frac{Ng^2\mu_B^2}{3k_BT} \frac{\sum_{s=0}^{2S} s(s+1)(2s+1)\exp\left[\frac{Js(s+1)}{2k_BT}\right]}{\sum_{s=0}^{2S} (2s+1)\exp\left[\frac{Js(s+1)}{2k_BT}\right]} + \frac{C_{def}}{T} \quad (1)$$

The solid curves in Figure 8 are the theoretical best fits of this model, obtained with $S=1/2$, $g=2.21$, $2J/k_B=-17.8$ K, and $C_{def}=0$ emu K mol^{-1} (fixed) for CoTTDPz, and with $S=2$, $g=2.40$, $2J/k_B=-9.1$ K, and $C_{def}=0.063$ emu K mol^{-1} (4.3%) for FeTTDPz. The experimental data are accurately reproduced by this dimer model.

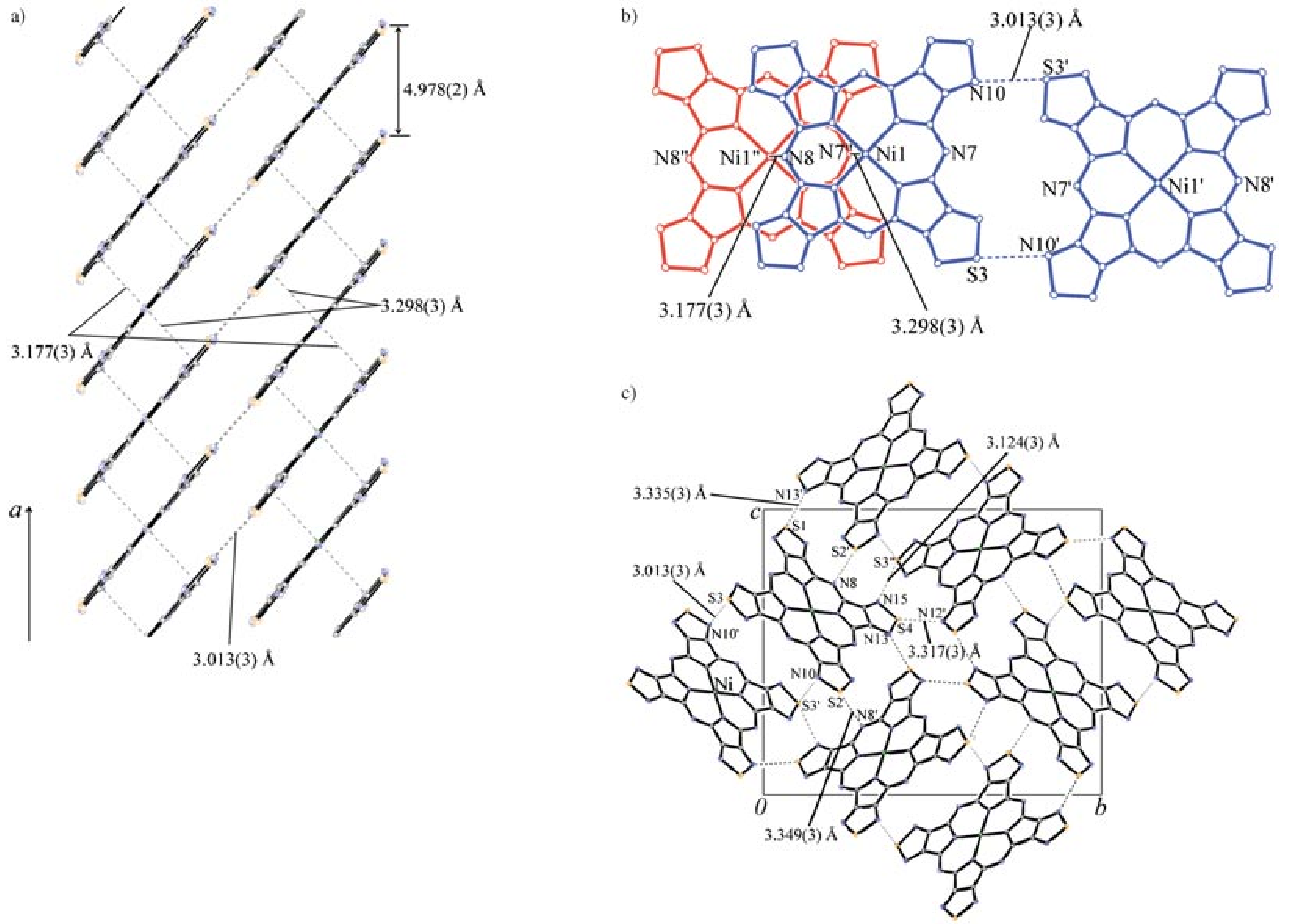

Figure 7. a) Side view of two-leg ladder structure, b) the intermolecular arrangements in the leg and row directions, and c) a projection of the crystal structure along the *a* axis of γ-NiTTDPz.

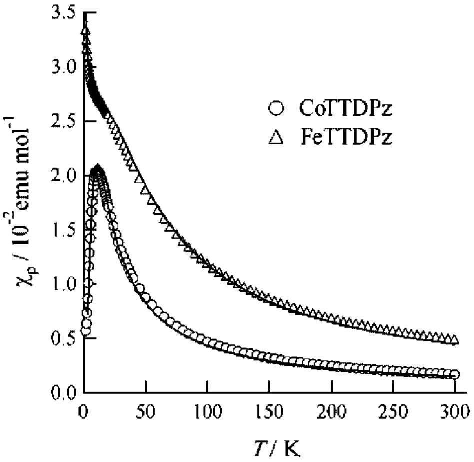

Figure 8. Temperature dependence of the paramagnetic susceptibility, χ_p, for β-FeTTDPz and β-CoTTDPz. The solid curves are the theoretical best fit of the dimer model.

The temperature dependence of χ_p for α′- and γ-CuTTDPz followed the Curie–Weiss law over the entire temperature range 2–300 K (not shown). The obtained parameters for the α′ phase are $C=0.41\pm0.03$ emu K mol^{-1} ($g=2.1$) and $\theta=0.6\pm0.8$ K, whereby C and θ are the Curie and Weiss constants, respectively. The large error for θ is caused by a shortage of sample of α′-CuTTDPz. The parameters for the γ phase are $C=0.42\pm0.04$ emu K mol^{-1} ($g=2.1$) and $\theta=0.7\pm0.2$ K. This Weiss constant suggests a weak ferromagnetic intermolecular interaction through the axial nitrogen atom, as in β-MnPc.[3] It is concluded that the magnetic interactions in α′- and γ-CuTTDPz are very weak due to long distances between the paramagnetic metal ions.

In contrast to the short intermolecular contacts, the magnetic exchange interactions are rather weak in the MTTDPz series. This is probably caused by the same reason as that in the MPc series; the intramolecular overlaps between the metal d orbitals and the porphyrazine π orbital (HOMO) are negligible. The d orbitals exhibit the gerade symmetry, in contrast to the ungerade symmetry for the HOMO. Therefore, the metal d orbitals are localized at the center of ring and the intermolecular magnetic exchange interactions become very weak.

Conclusion

In the present work, we obtained single crystals of the MTTDPz (M = H_2, Fe, Co, Ni, Cu, and Zn) series by means of sublimation under reduced pressure with continuous N_2 gas flow, and observed the three forms, α, β, and γ in their crystal structures. The structures were governed by three factors: axial coordination bonding, π–π interactions, and electrostatic S···N contacts, bringing about multi-dimensional networks. Although the magnetic exchange interactions were relatively weak, probably reflecting the long distances between metal ions, the obtained network structures suggest that after carrier doping these materials have good potential as three-dimensional conductors.

Experimental Section

Preparations of solvated MTTDPz ($M = H_2$, Mn, Fe, Co, Ni, Cu, Zn) were performed by a modification of the literature method.[10,11] The metal-free H_2TTDPz was obtained from MgTTDPz, which was synthesized by the reaction of 3,4-dicyano-1,2,5-thiadiazole with magnesium(II) propylate. The MTTDPz metal salts (M = Mn, Co, Ni, Zn) were obtained by reaction of H_2TTDPz with the corresponding hydrate metal(II) acetate in DMSO, while $Cu(py)_2$TTDPz and $Fe(py)_2$TTDPz were prepared by the same reaction in pyridine. All products were obtained in good yield and were confirmed by IR spectroscopy.

Single crystals were obtained (except for MnTTDPz) by sublimation of solvated MTTDPz under reduced pressure (about 10^{-3} bar) with continuous N_2 gas flow (50 mL min^{-1}) at 450–550 °C.

Magnetic measurements were carried out on a SQUID (Quantum Design MPMS XL) susceptometer. The experimental raw data were corrected for diamagnetism and the molar paramagnetic susceptibilities obtained.

X-ray diffraction data were collected with graphite-monochromated $Mo_{K\alpha}$ ($\lambda = 0.71073$ Å) radiation on a Mac Science DIP-3200 imaging plate diffractometer for MTTDPz ($M = H_2$, Fe, Co, Ni(α form), and Cu(γ form)) and on a Rigaku Mercury CCD diffractometer for MTTDPz (M = Ni(γ form), Cu(α′ form), and Zn). All structures were solved by a direct method using the SHELXS-97 program[22] and refined by successive differential Fourier syntheses and a full-matrix least-squares procedure using the SHELXL-97 program.[23] Anisotropic thermal factors were applied to all non-hydrogen atoms. Hydrogen atoms in H_2TTDPz were located by differential Fourier synthesis and were also refined.

CCDC-216083 (for H_2TTDPz), 236690 (for FeTTDPz), 216084 (for CoTTDPz), 236691 (for α-NiTTDPz), 236692 (for γ-NiTTDPz), 236688 (for α′-CuTTDPz), 236689 (for γ-CuTTDPz), 236687 (for ZnTTDPz) contain the supplementary crystallographic data for this paper. These data can be obtained free of charge via www.ccdc.cam.ac.uk/conts/retrieving.html (or from the Cambridge Crystallographic Data Centre, 12 Union Road, Cambridge CB21EZ, UK; fax: (+44)1223-336-033; or deposit@ccdc.cam.ac.uk).

Acknowledgement

The authors would like to thank Tamotsu Inabe and Claudio Ercolani for helpful discussions. This work was supported by the Grant-in-Aid for Scientific Research from the Ministry of Education, Science, and Culture, Japanese government.

[1] a) *Phthalocyanines: Properties and Applications*, *Vol. 4* (Eds.: C. C. Leznoff, A. B. P. Lever), VCH, New York, **1996**; b) *The Porphyrin Handbook*, *Vols. 17* and *19* (Eds.: K. M. Kadish, K. M. Smith, R. Guilard), Academic Press, New York, **2003**.

[2] *Sensors: A Comprehensive Survey*, *Vol. 2: Chemical and Biochemical Sensors*, *Part 1* (Eds.: W. Göpel, T. A. Jones, M. Kleitz, J. Lundström, T. Seiyama), VCH, Weinheim, **1991**.

[3] a) H. Miyoshi, H. Ohya-Nishiguchi, Y. Deguchi, *Bull. Chem. Soc. Jpn.* **1973**, *46*, 2724–2728; b) K. Awaga, Y. Maruyama, *Phys. Rev. B* **1991**, *44*, 2589–2594.

[4] a) C. G. Barraclough, R. L. Martin, S. Mitra, R. C. Sherwood, *J. Chem. Phys.* **1970**, *53*, 1643–1648; b) S. Mitra, A. Gregson, W. Hatfield, R. Weller, *Inorg. Chem.* **1983**, *22*, 1729–1732; c) M. Evangelisti, J. Bartolomé, L. J. de Jongh, G. Filoti, *Phys. Rev. B* **2002**, *66*, 144410.

[5] N. Ishikawa, M. Sugita, T. Ishikawa, S. Koshihara, Y. Kaizu, *J. Am. Chem. Soc.* **2003**, *125*, 8694–8695.

[6] J. M. Robertson, *Organic Crystals and Molecules*, Cornell University Press, New York, **1953**.

[7] F. H. Moser, A. L. Thomas, *Phthalocyanine compounds*, Reinhold Publishing Corp., New York, **1963**.

[8] T. Inabe, Y. Maruyama, *Bull. Chem. Soc. Jpn.* **1990**, *63*, 2273–2280.

[9] a) M. Matsuda, T. Asari, T. Naito, T. Inabe, N. Hanasaki, H. Tajima, *Bull. Chem. Soc. Jpn.* **2003**, *76*, 1935–1940; b) T. Inabe, *J. Porphyrins Phthalocyanines*, **2001**, *5*, 3–12, and references therein.

[10] P. A. Stuzhin, E. M. Bauer, C. Ercolani, *Inorg. Chem.* **1998**, *37*, 1533–1539.

[11] E. M. Bauer, D. Cardarrilli, C. Ercolani, P. A. Stuzhin, U. Russo, *Inorg. Chem.* **1999**, *38*, 6114–6120.

[12] M. P. Donzello, C. Ercolani, A. A. Gaberkorn, E. V. Kudrik, M. Meneghetti, G. Marcolongo, C. Rizzoli, P. A. Stuzhin, *Chem. Eur. J.* **2003**, *9*, 4009–4024.

[13] E. V. Kudrik, E. M. Bauer, C. Ercolani, A. Chiesi-Villa, C. Rizzoli, A. Gaberkorn, P. A. Stuzhin, *Mendeleev Commun.* **2001**, 45–47.

[14] M. Fujimori, Y. Suzuki, H. Yoshikawa, K. Awaga, *Angew. Chem.* **2003**, *115*, 6043–6045; *Angew. Chem. Int. Ed*, **2003**, *42*, 5863–5865.

[15] a) D. E. Hooks, T. Fritz, M. D. Ward, *Adv. Mater.* **2001**, *13*, 227–241; b) A. Yamashita, T. Hayashi, *Adv. Mater.* **1996**, *8*, 791–794, and references therein.

[16] Y. Iyechika, K. Yakushi, I. Ikemoto, H. Kuroda, *Acta Crystallogr. Sect. B* **1982**, *38*, 766–770.

[17] R. Kubiak and J. Janczak, *J. Alloys Compd.* **1992**, *189*, 107–111.

[18] a) T. Kobayashi, T. Ashida, N. Uyeda, E. Suito, M. Kakudo, *Bull. Chem. Soc. Jpn.* **1971**, *44*, 2095–2103; b) M. Mossoyan-Deneux, D. Benlian, M. Pierrot, A. Fournel, J. P. Sorbier, *Inorg. Chem.* **1985**, *24*, 1878–1882.

[19] D. R. Tackley, G. Dent, W. E. Smith, *Phys. Chem. Chem. Phys.* **2001**, *3*, 1419–1426.

[20] M. J. Cook, A. Jafari-Fini, *J. Mater. Chem.* **1997**, *7*, 2327–2329.

[21] O. Kahn, *Molecular Magnetism*, VCH, Weinheim, **1993**.

[22] Sheldrick, G. M. SHELXS-97: Program for crystal structure solution, University of Göttingen (Germany), **1997**.

[23] Sheldrick, G. M. SHELXL-97: Program for crystal structure refinement, University of Göttingen (Germany), **1997**.

Received: April 22, 2004